

Efficient two-photon-resonant frequency conversion in mercury: the effects of amplified spontaneous emission

A. V. Smith, G. R. Hadley, P. Esherick, and W. J. Alford

Sandia National Laboratories, Albuquerque, New Mexico 87185

Received April 14, 1987; accepted June 12, 1987

Numerical modeling of two-photon-resonant sum-frequency mixing in mercury vapor predicts efficiencies >10% for generation of 130.2-nm oxygen resonance light. The modeling indicates that power broadening of the two-photon resonance due to amplified spontaneous emission from the pumped level strongly influences the mixing process. Measurements of the broadening and the efficiencies for difference-frequency mixing are presented as a check of the model calculations.

In recent years a number of experimental¹⁻³ results have indicated that two-photon-resonant frequency mixing in Hg vapor can be quite efficient. In focused beam geometries and using typical laboratory lasers, efficiencies approaching 1% have been demonstrated. Our goal is to achieve efficiencies of several percent at the atomic-oxygen resonance wavelength of 130.2 nm in a system scalable to high energies. Scalability precludes use of tightly focused beams, so our approach is to substitute collimated beams with long interaction lengths and relatively low input intensities for the more customary high intensities and short interaction lengths. This has the added advantage of permitting realistic modeling of the mixing process.

In the focused case, peak intensities are 10^{10} W/cm² or greater. At these intensities, effects such as ac Stark shifts, photoionization broadening of the two-photon resonance, saturation of the two-photon resonance, nonlinear contributions to the refractive index, and population transfer make accurate modeling difficult. At sufficiently low intensities, most of these effects will become unimportant. The questions that we address here are these: What efficiency can be predicted for a scalable system, and what are the efficiency-limiting processes?

We previously reported⁴⁻⁶ measurements of those oscillator strengths of Hg that are important in calculating mixing efficiencies when one of the 7S states is two-photon resonant. Based on these values, we find that the effects listed above, with the exception of population transfer, should be negligible at input intensities less than 3×10^6 W/cm². Ignoring any effect associated with population transfer, we predict a mixing efficiency of 10% (for input intensities below this limit) with a Hg column density of only 265 Torr cm (details of the modeling are discussed below). However, under these conditions population transfer to the 7¹S level would lead to an amplified spontaneous emission (ASE) intensity of 112 kW/cm² if all the atoms were stimulated to emit at 1014 nm, the wavelength of the 7¹S-6¹P transition. This intensity would lead to substantial power broadening of the lasing transition. Power broadening would, in turn, alter the two-photon-resonant profile and, consequently, the mixing process.

We have examined this power broadening and its effect on frequency mixing by studying two-photon-resonant difference-frequency mixing using narrow-bandwidth (<0.01 cm⁻¹) pulsed lasers. Two equal-energy photons of 313-nm wavelength are resonant with the 6¹S-7¹S transition. They are generated by pulse amplifying a cw dye laser at 626 nm, using dye amplifiers pumped by the 10-nsec-duration second-harmonic pulses from a single-frequency, injection-locked Nd:YAG laser.⁷ The resulting narrow-bandwidth light at 626 nm is frequency doubled. The second-harmonic light from the Nd:YAG laser (532 nm) supplies the third wave for difference-frequency mixing in Hg to generate light at 221.6 nm.

The Hg is contained in a heat-pipe oven⁴ and has a density of 3.5 Torr and a column length of 35 cm. Index matching is achieved by crossing the collimated input beams at a slight angle.⁴ We measure the input intensities, the 221.6-nm difference-frequency intensity, and the ASE intensities at 1014 nm (7¹S-6¹P) and 407.9 nm (7¹S-6³P₁). We find that the 1014-nm pulse has a time dependence that follows the pump pulse. The 407.9-nm ASE occurs only at the trailing edge of the pump pulse, after the 1014-nm pulse terminates, and thus has no effect on the mixing process.

Figure 1(a) shows a plot of the difference-frequency signal as the 313-nm light is scanned across the 6¹S-7¹S transition at low intensity. In this case ASE is absent and the structure is due to the isotope shifts in the normal isotopic mixture of Hg.^{6,8} Figures 1(b) and 1(c) show the difference-frequency signal for successively higher intensities of the 313-nm pump light. Here ASE is present and broadens the individual lines until they merge into a continuous spectrum.

We model the mixing process by numerically integrating the coupled differential equations describing the growth of the four mixing waves. These equations can be found in Ref. 9, for example, and are of the form

$$\frac{dE_4}{dz} = iC\omega_4NL \left[\frac{\chi_m E_1 E_2 E_3}{\Delta - i\Gamma/2} \exp(-i\Delta kz) + \frac{\chi_r E_4 |E_3|^2}{\Delta - i\Gamma/2} \right] + \frac{i}{2k_4} \nabla_{\perp}^2 E_4, \quad (1)$$

where $(\chi_m)/(\Delta - i\Gamma/2)$ is the third-order nonlinear

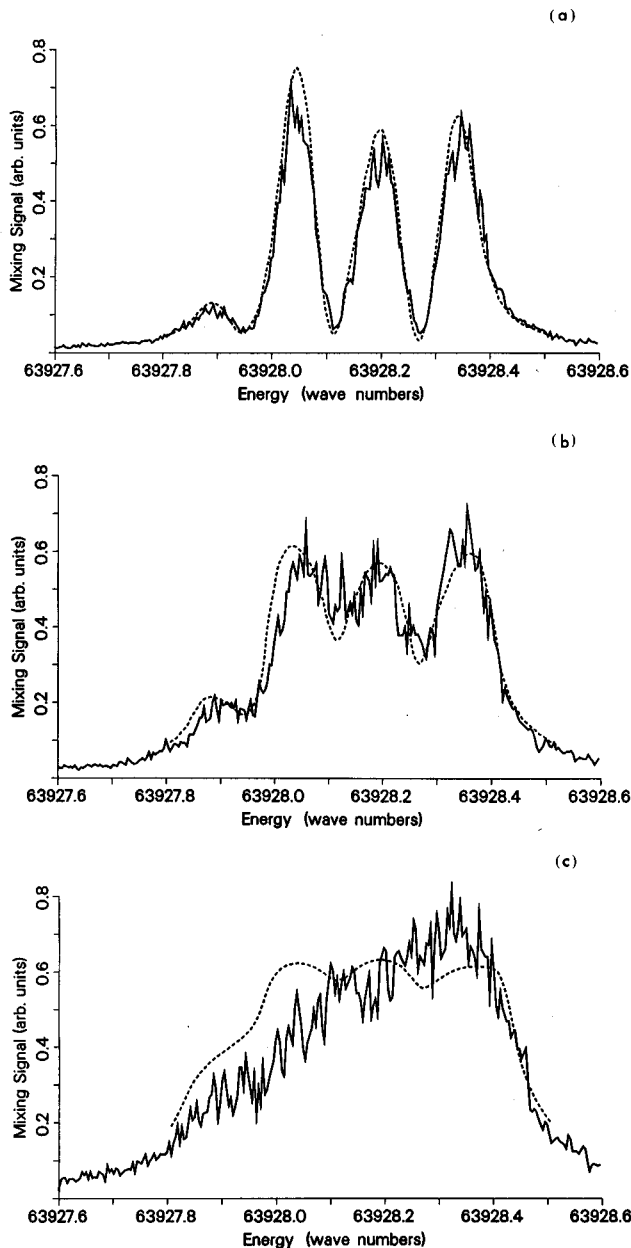


Fig. 1. Difference-frequency signal (222 nm) as the two-photon resonance is scanned using on-axis 313-nm intensities of (a) 4.8, (b) 1.6, and (c) 0.5 MW/cm². The dashed curves are computed using the model described in text.

susceptibility associated with four-wave mixing and $(\chi_r)/(\Delta - i\Gamma/2)$ is the susceptibility associated with Raman conversion of wave four to wave three in the case of sum-frequency mixing or with two-photon absorption in the case of difference-frequency mixing. The quantity Δ is the detuning from the two-photon resonance, and Γ is the resonance linewidth. The E_i 's are electric field amplitudes, and Δk is the index mismatch, assumed to be zero here. We assume square temporal pulses of 1-nsec duration and unfocused Gaussian transverse beam profiles. Transient behavior of the nonlinear susceptibilities is ignored, and thus we use steady-state susceptibilities. The resulting predicted curves for the difference-frequency mix-

ing experiment, scaled vertically to fit the data, are shown as the dashed curves in Fig. 1. The isotope and hyperfine structure is obtained from Ref. 8.

In the low-intensity case (no ASE), the resonance denominators in Eq. (1) are replaced with the result of Doppler averaging the weighted and shifted isotopic distribution of resonant denominators⁶ appropriate for the normal Hg isotope mixture. At higher pump intensities, where power broadening becomes significant, we replace the Doppler width with $[(\Delta\omega_D)^2 + (\Delta\omega_P)^2]^{1/2}$, where $\Delta\omega_D$ is the Doppler width and $\Delta\omega_P$ is the Rabi width or power-broadened width associated with the ASE. In calculating the ASE intensity, we assume that all atoms pumped to the 7^1S level are promptly stimulated to emit at 1.014 μm and add to the downstream ASE intensity. The associated power-broadened width is calculated from the known oscillator strength⁵ of the 7^1S - 6^1P transition using

$$\Delta\omega_P = 1.6 \times 10^{-3} (I_{\text{ASE}})^{1/2}, \quad (2)$$

where $\Delta\omega_P$ is in inverse centimeters and I_{ASE} is in watts per square centimeter.

With a single resonance ASE would probably split the 7^1S into a Rabi doublet. The situation is much more complex in the case considered here, however, because there are ten ASE wavelengths associated with the seven Hg isotopes. The ten lines near 1014 nm are spread over a range of about 0.25 cm⁻¹, but all isotopes have at least one component in a central cluster of width 0.07 cm⁻¹. Since the Doppler width is 0.01 cm⁻¹, there is considerable overlap among the Doppler-broadened lines. Thus the power splittings and power shifts of each isotopic two-photon resonance will depend on the complex ASE spectrum. Because of the difficulty of treating this complex process exactly, we make the simplifying assumption that 1014-nm ASE equally broadens each isotopic two-photon resonance with the value calculated by Eq. (2). The validity of this assumption is borne out by the good agreement in Figs. 1(b) and 1(c) between the calculated and measured two-photon-resonance line shapes in the strong-pump cases. Furthermore, the calculated mixing efficiencies agree with the observed efficiencies within the approximate experimental uncertainty of a factor of 2.

Having validated our model in the case of difference-frequency mixing, we now present the results of similar calculations performed to predict the result of sum-frequency mixing. The efficiency of difference-frequency production was rather low at $\approx 10^{-4}$. For 130.2-nm generation, we will show that much higher efficiencies can be achieved. This is due to the larger susceptibilities in this case and also to the use of much larger Hg-column densities.

From Ref. 6, the input wavelengths necessary to index match parallel input beams for 130.2-nm generation are 255.0, 404.6, and 777.2 nm. The importance of ASE is illustrated in Fig. 2, which contrasts this mixing process with ASE omitted [Fig. 2(a)] and included [Fig. 2(b)]. These plots show the power in each of the four waves as a function of position in the Hg cell. The strong saturation evident in Fig. 2(a) is due to an interference effect among the four waves and will

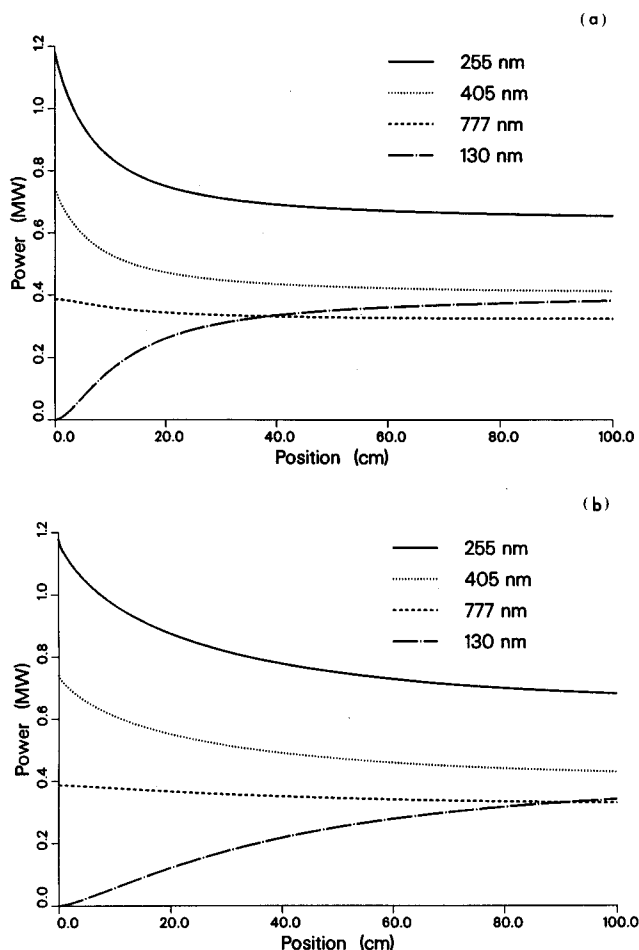


Fig. 2. Power in each of the four waves as a function of position in the Hg cell: (a) with no ASE and (b) with ASE. The Hg density is $6 \times 10^{17}/\text{cm}^3$. Gaussian beam radii at the input window are 0.5 cm ($1/e$ field).

be discussed in a later paper. This saturation limits the ultimate on-resonance mixing efficiency in both cases. However, a comparison of Fig. 2(a) with Fig. 2(b) shows that broadening of the two-photon resonance effectively lowers the nonlinear susceptibilities in the mixing equations as the waves propagate through the cell. This effect leads to the requirement of higher input intensities or higher Hg densities than would be the case in the absence of ASE in order to achieve a given mixing efficiency. Even so, efficiencies exceeding 10% are predicted for reasonable input intensities and Hg densities.

The calculations indicate that no serious transverse amplitude distortions of the waves occur. The profiles of the four waves are computed at the exit window of the cell and show that the 130.2-nm wave is nearly Gaussian in transverse profile. This profile indicates

that nonlinear refractive-index effects associated with the two-photon resonance are not a problem here.

We neglect the influence of the $6P$ population on Δk in these calculations. Resonance radiation trapping makes the effective lifetime of the 6^1P level considerably longer than the pulse length of 1 nsec, so we assume that all pumped atoms end up in the 6^1P level. From the predicted populations, however, the change in Δk is expected to be negligible. For longer pulse lengths, the population buildup will be greater, so this problem might become important.

One interesting consequence of the strong broadening in the presence of ASE is that little is gained by using isotopically enriched Hg for mixing. When the ASE broadening is greater than the isotope shifts, all the isotopes can contribute in the mixing process.

In conclusion, we have demonstrated the role of ASE in a two-photon-resonant frequency mixing process and presented a satisfactory model for the case of the $7S$ resonance in Hg. The primary effect of ASE seems to be a lowering of the effective Hg density. However, we have shown that impressive mixing efficiencies may still be possible for generation of 130.2-nm light by mixing in Hg. For a Hg column of 850 Torr cm and input intensities of 3, 2, and 1 MW/cm^2 at the center of the Gaussian input beams at 225.0, 404.6, and 777.2 nm, respectively, we predict an efficiency of 11%. Preliminary results from continuing efforts in modeling of the mixing process suggest that considerably greater efficiencies should be possible by detuning slightly from the two-photon resonance.

This research was performed at Sandia National Laboratories and supported by the U.S. Department of Energy under contract DE-AC04-76DP00789 for the Office of Basic Energy Sciences.

References

1. R. Mahon and F. S. Tomkins, *IEEE J. Quantum Electron.* **QE-18**, 913 (1982).
2. R. Hilbig and R. Wallenstein, *IEEE J. Quantum Electron.* **QE-19**, 1759 (1983).
3. P. R. Herman and B. P. Stoicheff, *Opt. Lett.* **10**, 502 (1985).
4. A. V. Smith and W. J. Alford, *Phys. Rev. A* **33**, 3172 (1986).
5. W. J. Alford and A. V. Smith, "Measured third-order susceptibility and excited-state oscillator strengths for atomic mercury," submitted to *Phys. Rev. A*.
6. A. V. Smith and W. J. Alford, "A practical guide for $7S$ resonant frequency mixing in Hg: generation of light in the 230–185- and 140–120-nm ranges," submitted to *J. Opt. Soc. Am. B*.
7. P. Esherick and A. Owyong, *J. Opt. Soc. Am. B*, **4**, 41 (1987).
8. S. Gerstenkorn, J. J. Labarthe, and J. Vergès, *Phys. Scr.* **15**, 167 (1977).
9. J. F. Reintjes, *Nonlinear Optical Parametric Processes in Liquids and Gases* (Academic, New York, 1984).